



Title	Electrical Characteristics of Lightly-Doped Si Films Crystallized by Thermal Plasma Jet Irradiation
Author(s)	Yorimoto, T.; Higashi, S.; Kaku, H.; Okada, T.; Murakami, H.; Miyazaki, S.; Maki, M.; Sameshima, T.
Citation	Transactions of the Materials Research Society of Japan, 32(2): 465-468
Issue Date	2007
URL	http://hdl.handle.net/20.500.12000/47347
Rights	©2020 MRS-J. All Rights Reserved.

Electrical Characteristics of Lightly-Doped Si Films Crystallized by Thermal Plasma Jet Irradiation

T.Yorimoto, S.Higashi, H.Kaku, T.Okada, H.Murakami,
S.Miyazaki, M.Maki* and T.Sameshima*

Graduate School of Advanced Sciences of Matter, Hiroshima University,
Kagamiyama 1-3-1, Higashi-Hiroshima

Fax: 81-82-422-7038, e-mail: semicon@hiroshima-u.ac.jp

*Tokyo University of Agriculture & Technology, Nakamachi 2-24-16 Koganei

50-nm-thick amorphous Si films doped with $4.3 \times 10^{17} \text{ cm}^{-3}$ phosphorus atoms were crystallized by thermal plasma jet (TPJ) irradiation. The electrical conductivity (σ) of the crystallized films ranges from $1.2 \times 10^{-5} \sim 1.7 \times 10^{-2} \text{ S/cm}$, while Si films crystallized by excimer laser annealing (ELA) show much smaller σ of $1.6 \sim 4.5 \times 10^{-6} \text{ S/cm}$ regardless of laser fluence. This result can be interpreted that the defect density in the TPJ crystallized films is much smaller than that in ELA Si films. By treating the films with hydrogen plasma for 60 s at 250 °C, σ of TPJ crystallized films increased to $1.4 \times 10^{-2} \sim 1.1 \text{ S/cm}$, while it was $3.0 \times 10^{-6} \sim 6.5 \times 10^{-3} \text{ S/cm}$ in the case of films crystallized by ELA. This result indicates that a short period hydrogenation is effective to improve the electrical characteristics of TPJ crystallized Si films.

Key words: thermal plasma jet, crystallization, polycrystalline Si, excimer laser, thin film transistor

1. INTRODUCTION

Application of ultrarapid thermal annealing (URTA) to crystallization of amorphous Si (a-Si) films is one of the key process technologies for the fabrication of large area electronic devices such as solar cells and thin film transistors (TFTs). We have applied thermal plasma jet (TPJ) to perform URTA of quartz substrate surface within millisecond, and reported the crystallization of a-Si films [1]. We have demonstrated its feasibility as obtained from good TFT performance such as the maximum field effect mobility of $70 \text{ cm}^2/\text{Vs}$ and threshold voltage of 3.3 V [2]. For the further improvement of TFT performance, control of defect density in the polycrystalline Si (poly-Si) films is one of the most important technological issues. In poly-Si films, it is reported that defects such as dangling bonds are localized at grain boundary [3,4]. Such defects form gap states and work as carrier trap sites. Therefore, the carrier concentration in doped-poly-Si films has strong dependence on the doping concentration. In this work, we have evaluated the σ of lightly-doped Si films crystallized by TPJ and ELA. By performing doping so that the dopant concentration is comparable to the defect density, one can observe significant difference of σ from TPJ and ELA crystallized poly-Si films. It is demonstrated that the defect density in TPJ crystallized Si films is

much smaller than that in ELA Si films.

2. EXPERIMENTAL

Amorphous Si films of 50 nm thickness were formed by low pressure chemical vapor deposition (LPCVD) using Si_2H_6 on quartz substrates at 425 °C. Capping SiO_2 films with the thickness of 75 nm were formed by plasma enhanced chemical vapor deposition (PECVD). Phosphorus atoms were implanted into the films with the dose amount of $5.0 \times 10^{12} \text{ cm}^{-2}$ and the acceleration energy of 70 keV. The average phosphorus concentration in the a-Si film is estimated to be $4.3 \times 10^{17} \text{ cm}^{-3}$. After removing the capping SiO_2 layer, the lightly doped a-Si films were crystallized by TPJ under the power input to the plasma source (P) of 2.04 to 2.10 kW and scanning speed (v) of 350 to 900 mm/s (see Fig.1). The distance between the plasma source and substrates (d) was set at 3 to 5 mm. In order to measure the temporal evolution of substrate temperature during the TPJ annealing, the reflectivity of the quartz substrate was measured from the backside using a probe cw laser as shown in Fig.1 [5]. On the basis of the transient temperature measurement, T_{max} is defined as the maximum surface temperature during the TPJ annealing. The annealing duration (t_a) is defined by the period during the surface temperature exceeds the 90 % of T_{max} . For comparison, σ of

lightly doped Si films crystallized by ELA at laser energy densities ranging from 270 to 402 mJ/cm² was measured. The crystallinity of the films was evaluated by Raman scattering spectroscopy, and the surface morphology was observed by atomic force microscopy (AFM). In order to reduce the defect density in the poly-Si films, hydrogen plasma treatment was performed at 250 °C for 60 s, under the flow rate of 100 % H₂ gas of 130 sccm, pressure of 130 Pa, and input power of 30 W.

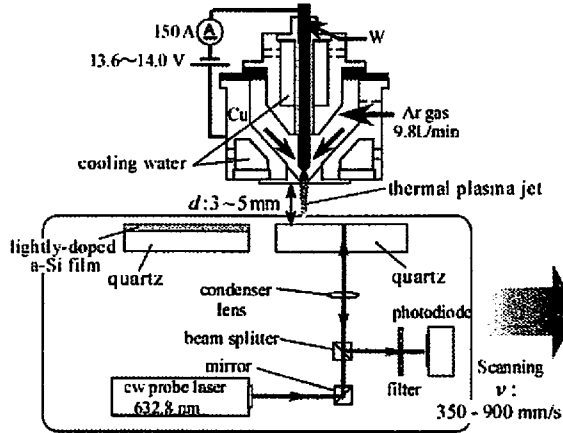


Fig.1 Schematic diagram of TPJ annealing of lightly-doped a-Si films. Transient reflectivity was measured by irradiating the sample with a cw probe laser from the backside of the substrate.

3. RESULTS AND DISCUSSION

Figure 2 shows the σ of Si films crystallized by TPJ under the condition of $d = 3$ to 5 mm and $v = 350$ to 900 mm/s. In Fig.2, σ is plotted as functions of T_{max} measured during TPJ annealing. σ increases with T_{max} , and it reaches to 1.7×10^{-2} S/cm by annealing the film with d of 5 mm and v of 350 mm/s. This result indicates that the defect density in the Si films decreases with TPJ annealing temperature. Figure 3 shows the σ of Si films crystallized by TPJ with d of 4 mm and T_{max} of 1340, 1480, 1525 K, respectively, as functions of reciprocal temperature ($1000/T$). Here, T is the temperature of the samples in the σ measurement. The activation energy is decreased from 0.58 to 0.26 eV with increasing T_{max} from 1340 to 1525 K. This result indicates that the carrier concentration in Si films increases and Fermi level (E_F) approaches to the conduction band with increasing T_{max} from 1340 to 1525 K. Next, we focused on films indicated by (a) ~ (c) in Fig.2. In these films, σ is greatly different although the films are crystallized with almost same T_{max} of

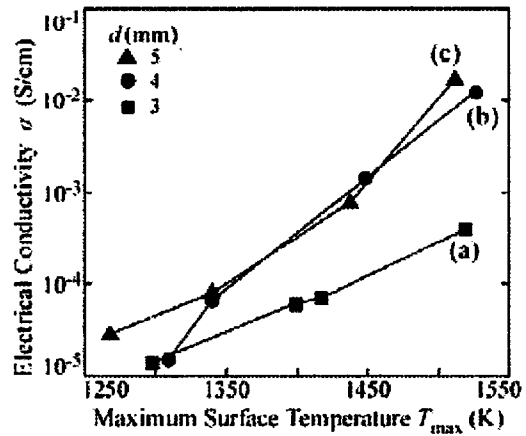


Fig.2 σ of lightly-doped Si films crystallized by TPJ as functions of T_{max} .

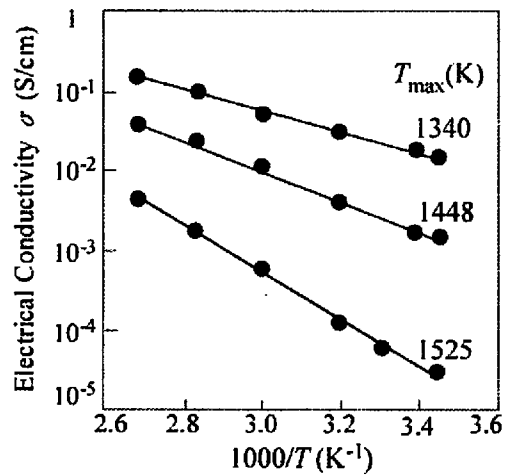


Fig.3 σ of lightly-doped Si films crystallized by TPJ as functions of reciprocal temperature.

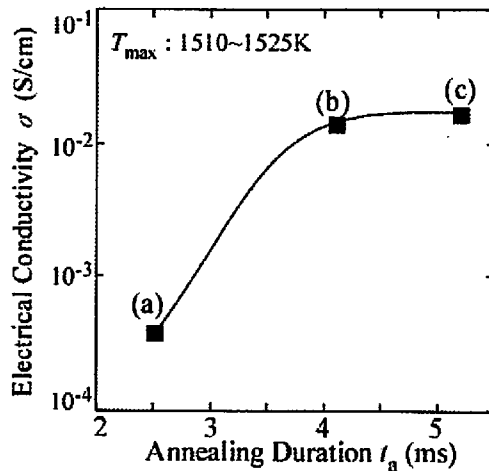


Fig.4 σ of lightly-doped Si films as a function of t_a .

1510 ~ 1525 K. In figure 4, the σ of these films is plotted as a function of t_a . σ increased from 3.9×10^{-4} to 1.7×10^{-2} S/cm as t_a increased from 2.5 to 5.2 ms. Figure 5 shows Raman scattering spectra and AFM images of samples (a) ~ (c) in Fig.4. The surface roughness (root-mean-square value) and the average grain size are 0.4 – 0.5 nm and about 25 nm, respectively, and no significant difference is observed in their AFM images. On the other hand, crystallinity of the films is improved with increasing t_a , which indicates that the defects that generated during the solid phase crystallization (SPC) decreases with increasing t_a . These results suggest that the defect density of Si films crystallized by TPJ are dependent on both annealing temperature and duration.

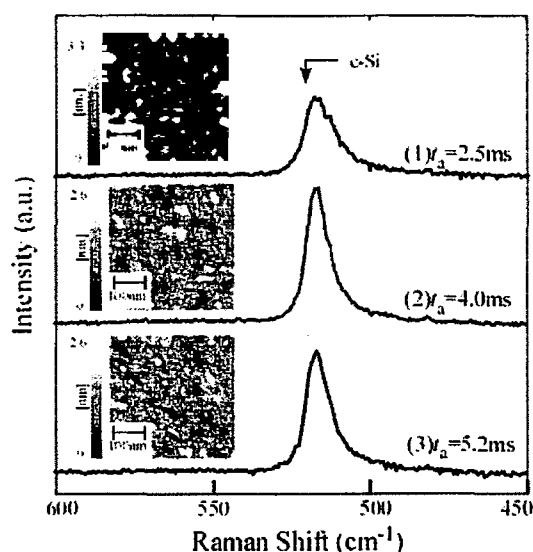


Fig.5 Raman scattering spectra and AFM images of Si films crystallized by TPJ under different t_a .

Figure 6 shows the σ of lightly-doped Si films crystallized by TPJ and ELA before and after hydrogen plasma treatment. The σ of samples crystallized by ELA before hydrogenation shows very low value of $1.6 \sim 4.5 \times 10^{-6}$ S/cm regardless of irradiated laser density, while that of TPJ crystallized Si films have much higher σ of $1.5 \times 10^{-5} \sim 1.4 \times 10^{-2}$ S/cm. This result indicates that the defect density in TPJ Si films is much lower than ELA films. Figure 7 shows the AFM images of samples (a) and (b) in Fig.6. The surface roughness of TPJ crystallized Si film is 0.4 nm, while it is 2.4 nm in ELA case. It should be noted that TPJ crystallized Si film has much higher σ although the grain size of ~ 25 nm is smaller compared to that of ~ 40 nm in ELA crystallized films. This indicates that defect density of TPJ

film localized at grain boundaries is significantly lower than that of ELA. This may due to the much longer annealing duration in the range of millisecond while it is significantly shorter in nanosecond range in the case of ELA. The σ of both films crystallized by TPJ and ELA remarkably increased after hydrogenation. The σ of Si films crystallized by ELA increased from 2.0×10^{-6} to 6.5×10^{-3} S/cm, and that of TPJ increased from 1.4×10^{-2} to 1.1 S/cm at maximum. This result is understood that the defects in as-crystallized films are terminated by hydrogen and trapped electron become free. It is understood that the effect of short period hydrogen plasma treatment remarkably improves σ of in TPJ films because of lower defect density in as-crystallized films compared to that of ELA case.

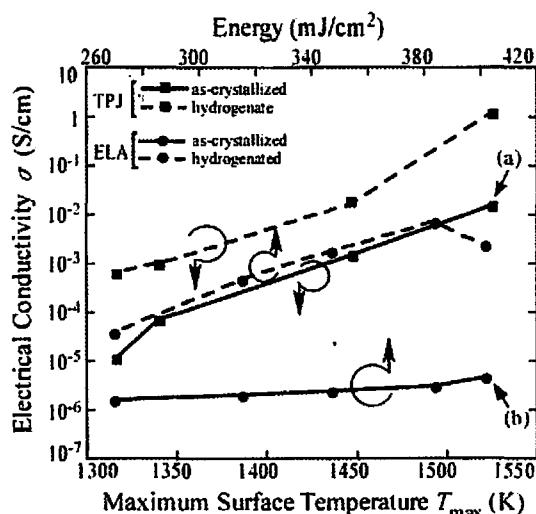


Fig.6 σ of Si films as-crystallized by TPJ and ELA and after hydrogenation.

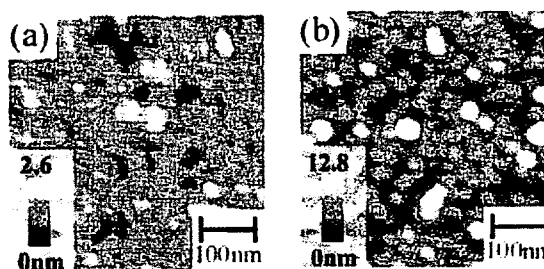


Fig.7 AFM images of Si films crystallized by (a)TPJ and (b)ELA.

4. CONCLUSIONS

The σ of Si film crystallized by TPJ increased from 1.5×10^{-5} to 1.4×10^{-2} S/cm with increasing T_{max} from 1316 to 1525 K. At the same T_{max} , the σ increased from 3.9×10^{-4} to 1.7×10^{-2} S/cm with

increasing t_a from 2.5 to 5.2 ms. The defect density in as-TPJ crystallized Si films depends on both annealing temperature and duration. After the hydrogen plasma treatment, the σ of ELA films increased from 2.0×10^{-6} to 6.5×10^{-3} S/cm, and the σ of films crystallized by TPJ increased from 1.4×10^{-2} to 1.1 S/cm. The defect density in TPJ crystallized Si film is much lower than that of ELA, which results in significant improvement in electrical performance with a short period hydrogenation.

ACKNOWLEDGEMENTS

A part of this work is supported by the Industrial Technology Research Grant Program in 2005 from New Energy and Industrial Technology Development Organization (NEDO) of Japan.

REFERENCES

- [1] H. Kaku, S. Higashi, H. Taniguchi, H. Murakami, and S. Miyazaki, *Appl. Surf. Sci.* 244 (2005) 8.
- [2] S. Higashi, H. Kaku, H. Murakami, S. Miyazaki, H. Watakabe, N. Ando and T. Sameshima, *Jpn. J. Appl. Phys.* 44 (2005) L108.
- [3] S. Higashi, K. Ozaki, K. Sakamoto, Y. Kano, and T. Sameshima., *Jpn. J. Appl. Phys.* 38 (1999) L857.
- [4] John Y.W. Seto, *J. Appl. Phys.* 46 (1975) 5247.
- [5] T. Okada, S. Higashi, H. Kaku, N. Koba, H. Murakami, S. Miyazaki, *Jpn. J. Appl. Phys.* 45 (2006) 4355.

(Received December 23, 2006; Accepted April 7, 2007)